



## Effects of Methotrexate on IL-6, VCAM-1 and NF Kappa B Expression in a Rat Model of Metabolic Syndrome

Nicolas F Renna<sup>1,2\*</sup>, Jesica M Ramirez<sup>3</sup>, Rodrigo D Garcia<sup>1</sup>, Emiliano A Diez<sup>2</sup> and Roberto M Miatello<sup>1,2</sup>

<sup>1</sup>Department of Pathology, School of Medicine, National University of Cuyo, Argentina

<sup>2</sup>Laboratory of Cardiovascular Physiopathology, Institute of Experimental Medicine and Biology of Cuyo Argentina

<sup>3</sup>Genetic Institute, National University of Cuyo, Argentina

\*Corresponding author: Nicolás Federico Renna, Facultad de Ciencias Médicas, Universidad Nacional de Cuyo Av. Libertador 80, Centro Universitario 5500- Mendoza, Argentina, Tel: +54-261-44494046, E-mail: nicolasrenna@fcm.uncu.edu.ar

### Abstract

**Background:** In this study, we used Methotrexate (Mtx) to examine the role of immunomodulation on the activation of IL-6 and VCAM-1, which could generate a microenvironment that supports cardiovascular remodelling.

**Methods:** Male WKY and SHR rats were separated into five groups: Control, FFR: WKY rats receiving a 10% (w/v) fructose solution during all 12 weeks, SHR, FFHR: SHR receiving a 10% (w/v) fructose solution during all 12 weeks and FFHR+Mtx (0,3 mg/kg intraperitoneal one injection per day week for 6 weeks) (n = 8 per group). Metabolic variables and systolic blood pressure were measured. Cardiac and vascular remodelling was also evaluated. To assess this, IL-6R and VCAM-1 immunostaining techniques were used.

**Results:** The FFHR experimental model developed metabolic syndrome, vascular and cardiac remodelling, and vascular inflammation because of increased expression of IL-6 and VCAM-1. Chronic treatment with Mtx completely or partially reversed the variables studied.

**Conclusions:** The results demonstrated an impact on immunomodulation after mtx treatment, which included a reduction in vascular inflammation and a favourable reduction in metabolic and structural parameters.

### Keywords

Fructose-fed hypertensive rats, Metabolic syndrome, Hypertension, Methotrexate, Vascular inflammation, Cytokines

### Introduction

Increasing evidence suggests that immune activation and inflammatory mediators may play a role in the development and progression of atherosclerosis. Several studies have shown that patients with some diseases characterized by inflammatory mediator activation, which rheumatoid arthritis (RA), presented accelerated atherosclerosis. RA is a systemic inflammatory disease and the most common cause of death is due to accelerated atherosclerosis,

especially coronary artery disease. The incidence of myocardial infarction is 30%-60% higher [1], and its onset in RA is approximately 10 years earlier [2,3]. The age- and sex-adjusted mortality rate for cardiovascular disease (CVD) in RA patients is 50%-100% higher than the rate in the general population [4]. Increased prevalence of diabetes, hypertension, hypercholesterolemia, and metabolic syndrome in RA could explain the increased mortality; however, RA alone is also responsible for the excess of cardiovascular morbidity and mortality [5]. The traditional atherosclerotic risk factors alone cannot explain the accelerated atherosclerosis in RA patients. Some studies have reported that chronic inflammation might play a major role in accelerated atherosclerosis [6]. Inflammation can cause abnormal lipid metabolism and also transform fatty streaks into unstable plaques. Additionally, there is evidence that atherosclerosis is an inflammatory disease [7].

The increased prevalence of coronary artery disease and the high CVD mortality rate results from chronic systemic inflammation and enhanced instability of atherosclerotic plaques. These factors, in addition to traditional CVD risk factors, are thought to impact RA [8]. RA patients treated with disease-modifying anti-rheumatic drugs (DMARDs) showed a reduced risk for CVD compared to those without DMARDs [9]. In a case control study, Suissa, et al. reported that RA patients treated with DMARDs displayed a decreased prevalence of acute myocardial infarction [10].

We used methotrexate to examine the role of immunomodulation on the activation of different molecular inflammatory cytokines that could generate a microenvironment that supports cardiovascular remodelling.

### Methods

#### Animals and experimental design

All procedures were performed according to institutional guidelines for animal experimentation. The protocol was submitted and approved by the Institutional Committee for Laboratory Animal Use and Care (ICLAUC) at the School of Medicine-UNCuyo. Thirty-

day-old male Wistar Kyoto (WKY) and spontaneously hypertensive rats (SHR) were fed a standard commercial chow diet ad libitum. All rats were housed in a room under controlled temperature (20°C) and humidity conditions with a 12-hour light/dark cycle during the 12-week experimental period. Metotrexate (Mtx/Metotrexate Mtx) was administered to the following groups during the last six weeks of the study.

I-Control (W): WKY rats receiving food and drinking water (DW) ad libitum;

II-SHR receiving food and DW ad libitum;

III-Fructose-fed rats (FFR): WKY rats receiving a 10% (w/v) fructose (Parafarm, Buenos Aires, Argentina) solution in the DW during all 12 weeks,

IV-Fructose-fed hypertensive rats (FFHR): SHR rats receiving a 10% (w/v) fructose solution in the DW during all 12 weeks;

V- FFHR+Mx: FFHR receiving 0.3 mg/kg of Mtx by intraperitoneal (i.p.) administration once a week for 4 weeks.

MTX is a folic acid antagonist on the basis of its competitive binding to dihydrofolate reductase, an enzyme involved in de novo synthetic pathways for purine and pyrimidine precursors of DNA and RNA required for cell proliferation. Therefore, Mtx has been used extensively for treatment of neoplastic diseases in doses of 20 to 250 mg/kg. Low doses of Mtx were used (0.1-0.3 mg/dL once week for 4-6 weeks) because it has been reported anti-atherosclerotic effects via its anti-inflammatory actions.

At the end of the experimental period, the rats were euthanized with sodium pentobarbital (50 mg/Kg i.p.), blood samples were taken, and the arteries and organs were aseptically excised for measurements. At this dose, no gastrointestinal damage has been described. In the same way, the macroscopic revision of the gastric tissue was performed in random animals, and no lesions were found at this level.

### Systolic blood pressure measurement

The systolic blood pressure (SBP) was monitored indirectly in conscious, pre-warmed rats that were mildly restrained by the tail-cuff method and recorded on a Grass Model 7 polygraph (Grass Instruments Co., Quincy, MA, USA). The rats were habituated to the apparatus several times before measurement.

### Biochemical determinations

HOMA index and intra-peritoneal glucose tolerance test.

The fasting plasma insulin was assayed using the ACS: 180SE automated chemiluminescence system (Bayer, Germany). The plasma glucose levels were assayed using a commercial colorimetric method (Wiener Lab., Argentina). The HOMA was used as an index to measure the degree of insulin resistance. HOMA was calculated using the following formula:  $[\text{insulin } (\mu\text{U/mL}) \times \text{glucose (mmol/L)}] / 22.5$  [11].

Three days before the end of the experimental period, a glucose tolerance test (GTT) was performed. Rats were fasted overnight and were slightly anesthetized with pentobarbital. Then, glucose was administered (2 g/kg i.p.). Blood samples were taken by tail bleeding at 0, 30, 60, and 90 minutes after injection to determine the plasma glucose concentration. The total area under the curve was calculated as mmol/L/90 min.

### Assessment of the lipid profile

At the end of the experimental period, blood samples were drawn from the animals after fasting for 12 hours. The total plasma cholesterol, HDL cholesterol, and triglycerides were assessed using photocolourimetric enzymatic methods (Wiener Lab., Rosario, Argentina). The data are expressed in mmol/L.

### Oxidative stress determinations

Measurement of plasma thiobarbituric acid-reactive substances (TBARS).

To demonstrate the effect of increased oxidative stress at the vascular level, plasma lipid peroxidation was assessed by determining the TBARS concentration. This assay is based on the reaction between plasma malondialdehyde, a product of lipid peroxidation, and thiobarbituric acid, as previously described [8]. No correction for sample protein content was necessary because of the nature of sample [9].

### Measurement of vascular nad(p)h-oxidase activity

The lucigenin-derived chemiluminescence assay was used to determine the NAD(P)H-oxidase activity in a segment of the thoracic aorta, as previously described [8]. To assess NAD(P)H-oxidase activity, NADPH (500  $\mu\text{mol/L}$ ) was added, and chemiluminescence was immediately measured in a liquid scintillation counter (LKB Wallac Model 1219 Rack-Beta Scintillation Counter, Finland) set in the out-of-coincidence mode. Time-adjusted and normalized-to-tissue-weight scintillation counters were used for the calculations. The measurements were repeated in the absence and presence of diphenylene iodonium (DPI) (10<sup>-6</sup> mol/L), which inhibits flavin-containing enzymes, including NAD(P)H oxidase [10,12].

### Relative heart weight

To evaluate cardiac hypertrophy, we measured the relative heart weight (RHW). Briefly, the heart was separated from the great vessels, placed in a phosphate-buffered saline (PBS) solution, blotted with tissue paper to remove the blood, and weighed. The total heart weight was corrected according to the ratio between the heart weight (milligrams) and 100 grams of the total body weight before sacrifice.

### Tissue preservation

Tissue samples for histopathology were processed as previously reported [10]. Samples from all rats were used for these observations. Anesthetized animals were briefly perfused with PBS (298 mOsmol/KgH<sub>2</sub>O, pH 7.40, 4 °C) to remove the blood. The mesenteric arteries were perfused in vivo with the same solution through the mesenteric artery for 5 min. For the histological studies, the arteries were also perfused with a 4% paraformaldehyde solution for 10 min and fixed in paraffin wax. Five-micron-thick tissue slices were transversely cut across the mesenteric tissue on a microtome (Microm HM, Germany) and processed for histological studies. A similar procedure was applied for heart tissue preservation by aortic retrograde perfusion.

### Quantitative histomorphometry to determine cardiac hypertrophy

Histomorphological analyses were conducted on slices from the outer (free) wall of the left ventricle (LV) of the heart. Estimations of the cardiomyocyte area were made from sections stained with Masson trichrome solution. Areas with transverse sections of myofibres were selected. The contour of the fibres was then drawn manually. The total cardiomyocyte area was expressed in square micrometres ( $\mu\text{m}^2$ ).

### Arterial structure

The medial layers of the mesenteric arteries were measured to assess changes in the structure of the arterial walls. The slices were dyed and examined as previously described [10]. Non-transverse sectioned arteries were excluded from the investigation. Next, the lumen-to-media ratio (i.e., the ratio of the internal diameter to the medial (L/M) thickness) was calculated. Fifty slices from each animal were processed and analysed to obtain an average value for each rat. The average values were then used for the final analysis.

### Immunohistochemistry (IHC) and digital confocal microscopy

A rabbit antibody against the C-terminus of rat NF- $\kappa\text{B}$  p65 subunit [Rel A] was obtained from Millipore International Inc. (AB1604b; Amsterdam, Netherlands), and a goat anti-rat VCAM-1 (C-19) antibody was obtained from Santa Cruz Biotechnology Inc. (sc-1504; Santa Cruz USA). Tissue sections were cut at a 3- $\mu\text{m}$

**Table 1:** Metabolic and cardiovascular variables.

Variable	WKY	FFR	SHR	FFHR	FFHR+Mtx
Fasting glucose (mmol/L)	4.88 ± 0.1	6.44 ± 0.2 <sup>*</sup>	5.0 ± 0.2	6.5 ± 0.2 <sup>^</sup>	5.0 ± 0.1 <sup>''</sup>
Fasting triglycerides (mmol/L)	0.8 ± 0.0	1.9 ± 0.0 <sup>#</sup>	1.0 ± 0.0	1.9 ± 0.1 <sup>#</sup>	0.9 ± 0.2 <sup>''</sup>
HOMA (μU/mL insulin x mmol/L glucose) / 22.5	4.00 ± 0.2	11.0 ± 0.1 <sup>#</sup>	7.1 ± 0.15 <sup>^</sup>	15.1 ± 0.5 <sup>#^</sup>	4.50 ± 0.5 <sup>''</sup>
Area under glucose tolerance test curve (mmol / L / 90 min)	881 ± 64	1352 ± 21 <sup>#</sup>	1300 ± 35 <sup>^</sup>	1909 ± 51 <sup>#^</sup>	1005 ± 67 <sup>''</sup>
HDL cholesterol (mg/dl)	21.5 ± 0.3	13.2 ± 0.4 <sup>#</sup>	19 ± 1.0 <sup>*</sup>	11.6 ± 1.5 <sup>#^</sup>	18.2 ± 1.3 <sup>''</sup>
High-sensitivity C reactive Protein (mg/dL)	1.5 ± 0.1	3.5 ± 0.0	3.1 ± 0.1	4.5 ± 0.1 <sup>#^</sup>	0.9 ± 0.3 <sup>''</sup>
Systolic blood pressure (mmHg)					
Baseline	105 ± 3	102 ± 1.0	103 ± 1	105 ± 3	105 ± 2
6 weeks	110 ± 1.0	129 ± 2.0 <sup>^</sup>	165 ± 2 <sup>^</sup>	172 ± 3 <sup>#</sup>	170 ± 3 <sup>*</sup>
12 weeks	115 ± 1.3	139 ± 3.0 <sup>^</sup>	178 ± 1 <sup>#</sup>	185 ± 2 <sup>#^</sup>	135 ± 1.7 <sup>''</sup>

The above values correspond to metabolic and cardiovascular variables. Symbols indicate: <sup>\*</sup>p < 0.001 vs. WKY; <sup>^</sup>p < 0.001 vs. SHR; <sup>#</sup>p < 0.01 vs. FFR. <sup>''</sup> vs. FFHR.

**Table 2:** Oxidative stress and morphometric variables.

Variable	WKY	FFR	SHR	FFHR	FFHR+Mtx
NAD(P)H oxidase activity (counts/min/mg tissue)	40.5 ± 6	133 ± 5 <sup>^</sup>	160 ± 9.1 <sup>#</sup>	297 ± 9.1 <sup>#^</sup>	41 ± 5.1 <sup>''^</sup>
TBARS (μmol/L)	1 ± 0.1	2.2 ± 0.1 <sup>^</sup>	1.69 ± 0.1 <sup>^</sup>	2.8 ± 0.1 <sup>#^</sup>	1.0 ± 0.7 <sup>#^</sup>
Relative heart weight (mg/100 g body weight)	225 ± 4	290 ± 4 <sup>^</sup>	330 ± 1.8 <sup>#</sup>	400 ± 4 <sup>#^</sup>	290 ± 4 <sup>''</sup>
Myocardocyte area (μm <sup>2</sup> )	1682 ± 69	2066 ± 57 <sup>^</sup>	2222 ± 78 <sup>#</sup>	3242 ± 55 <sup>#^</sup>	1688 ± 34 <sup>''</sup>
Lumen/media relationship in mesenteric arteries	13.9 ± 0.3	10.2 ± 0.5 <sup>^</sup>	8.9 ± 0.6 <sup>#</sup>	8.45 ± 0.2 <sup>#</sup>	14.8 ± 2 <sup>''</sup>

The above values correspond to oxidative stress and morphometric variables. Symbols indicate: <sup>^</sup>p < 0.001 vs. WKY; <sup>^</sup>p < 0.001 vs. SHR; <sup>#</sup>p < 0.01 vs. FFR. <sup>''</sup> vs. FFHR.

thickness from paraffin-embedded blocks. The antibodies were diluted to 1:1000. The primary incubations were carried out for 1 hour at 21-22 °C, followed by six 5-min washes using PBS with Triton X-100. The secondary antibodies, anti-rabbit IgG TR and anti-goat IgG FITC (Sigma-Aldrich), were diluted in PBS alone according to the manufacturer's instructions.

The images were captured with Nikon EZ-C1 3.00 software on a Nikon Diaphot TMD microscope.

### SDS-PAGE and immunoblot analysis

The mesenteric tissue from each rat was washed in PBS, and the proteins were extracted in a cold extraction buffer (20 mM Tris-HCl, pH 7.4, 150 mM NaCl, 10% glycerol, 1% Triton X-100) and a protease inhibitor mixture (P2714, Sigma). The samples were sonicated for 15 s (three times with 10-s intervals), with a 30-min extraction for 30 min at 4 °C. The sample extracts were clarified by centrifugation at 14,000 × g for 20 min and used immediately or stored at -20 °C. The proteins were separated on 10% polyacrylamide gels and transferred to 0.22-μm nitrocellulose membranes (GE, Germany). Nonspecific reactivity was blocked by incubation for 1 h at room temperature in 5% non-fat dry milk dissolved in washing buffer (PBS, pH 7.6, 0.2% Tween 20). The blots were incubated with anti-p65, anti-VCAM-1 antibodies (0.2 μg/mL blocking solution) and anti-IL6R alpha (sc-660) rabbit IgG for 60 min at room temperature. Horseradish peroxidase-conjugated goat anti-rabbit-IgG and swine anti-goat-IgG were dissolved in blocking buffer and used as secondary antibodies (0.25 μg/mL, blots were incubated for 45 min at room temperature). Excess first and second antibodies were removed by washing five times for 5 min each time in blocking solution. Detection was accomplished with an enhanced chemiluminescence system (ABC, Dako System) and subsequent exposure to Kodak X-AR film (Eastman Kodak) for 5-30 s.

### Measurement of the concentration of high-sensitive C Reactive Protein (hs-CRP)

The plasma hs-CRP concentrations were measured using a turbidimetric assay (Bayer Advia 1650, AG Leverkusen). The data are expressed in mg/L.

### Reagents

Unless otherwise noted, all reagents were purchased from Sigma Chemical Co, MO, USA.

### Statistical and data analysis

The data are expressed as the mean ± SEM. The statistical significance of the comparisons between all groups was assessed by one-way ANOVA followed by a Bonferroni post-test. A two-sided p-value of less than 0.05 was considered significant.

### Results

#### Methotrexate improves metabolic indexes and blood pressure

Chronic administration of fructose induced several alterations that are considered in the cluster of risk factors that characterize MS. The comparison between the HOMA index and the areas under the GTT curve indicated that the FFR and FFHR developed glucose intolerance, as demonstrated by the significantly increased HOMA index and area values compared to the control rats (Table 1).

Furthermore, the animals in the FFR and FFHR groups also displayed significant differences in the levels of triglycerides and HDL-cholesterol when compared to the controls (Table 1). The SHR, FFR, and FFHR also displayed significant differences in the levels of hs-CRP when compared to the WKY rats. The FFHR group displayed higher hs-CRP levels than the other groups. Mtx reduced all of these variables to the levels observed in WKY rats (Table 1).

Table 1 also shows the time-course of the changes in SBP during the experimental period. By the sixth week, the SBP values of the FFHR and SHR groups were significantly increased compared to the control group, and there was an increase in pressure in the FFR group, which was lower but still significant. Treatment with Mtx did not return the SBP values to those of the control animals. These results on the value of blood pressure are statistically significant but not clinically significant because the reduction of this value was not less than 140 mmHg.

#### Methotrexate results in the recovery of the oxidative status

Table 2 indicates that NAD(P)H-oxidase activity and the plasma TBARS concentration was significantly higher in the aortas of FFHR when compared to those from the other groups. In previous studies the arterial eNOS activity in the FFHR group was significantly reduced, contributing to a decrease in the production and consequent bioavailability of nitric oxide (NO) [10,13-15].

Administration of Mtx effectively reduced superoxide production by reducing the activity of NAD(P)H oxidase and TBARS (Table 2), which normalized the endothelial oxidative status (Table 2).

## Methotrexate modifies cardiac and vascular hypertrophy

The RHW and myocardiocyte area was significantly higher in the FFR, SHR, and FFHR groups than in the control rats, demonstrating myocardial hypertrophy in these experimental models (Table 2). The FFHR group always displayed a significantly reduced L/M when compared to the corresponding arteries from the WKY group. This result was also observed in the FFR and SHR groups. Chronic treatment with Mtx significantly reduced myocardial hypertrophy and vascular remodelling in the FFHR model (Table 2).

## Methotrexate impacts vascular inflammation

The expression of NF- $\kappa$ B, VCAM-1, and IL-6R, products that actively participate in vascular inflammation, is shown in figure 1. Both molecules were detected by IHC. The expression of these molecules in the FFHR group increased significantly compared to the control group (W). The right panel shows a representative image of a WB for these proteins. The average optical density significantly increased in mesenteric artery homogenates from the FFHR and FFR groups compared to the controls. The distribution of the control protein load was similar for all groups. This work is the first to show an increase in the IL-6 alpha receptor in the vascular wall. This observation could explain vascular changes as well as the interaction with the renin-angiotensin system through different intracellular cascades.

Mtx reduced the activation and nuclear translocation of NF- $\kappa$ B (p65 fraction), VCAM-1 and IL-6 alpha receptor expression. This observation could be explained because in the FFHR group, nuclear factor NF- $\kappa$ B production was more important due to the production of superoxides as a result of the insulin-resistance status. This may also be a determining factor in the reduction of vascular remodelling, as previously shown.

## Discussion

In this article, we demonstrated that MTX reduces vascular inflammation that is accompanied by a reduction in metabolic and structural parameters.

In papers, as first noted in the Cholesterol and Recurrent Events (CARE) trial more than a decade ago, the benefits of pravastatin were particularly pronounced among patients with evidence of ongoing vascular inflammation. The AFCAPS/TexCAPS trial and JUPITER trial, tested the hypothesis that markers of inflammation can identify a group of patients who do not qualify for statin therapy because of normal lipid levels but who might nonetheless benefit from treatment. Further analyses indicated that the reduction in cardiovascular events derived from both the observed reduction in vascular inflammation, as measured by hsCRP, and from reductions in LDL-C.

The Cardiovascular Inflammation Reduction Trial's primary aim tests this hypothesis, a matter of considerable clinical therapeutic as well as mechanistic biological interest (CIRT, ClinicaTrials.gov NCT01594333). Before CARE results, novel approaches to preventing the macrovascular complications of insulin resistance and diabetes are urgently needed. Patients with type 2 diabetes or the metabolic syndrome also have a high prevalence of subclinical vascular inflammation, as determined by high levels of circulating inflammatory biomarkers. Indeed, some investigators have hypothesized that alterations in innate immunity underlie insulin resistance and diabetes

Emerging evidence raises the hypothesis that at least part of the anti-inflammatory and atheroprotective effects of low doses of Mtx (LDM) may result from increased adenosine release and subsequent agonism of the adenosine A2A receptor. Stimulation of this receptor

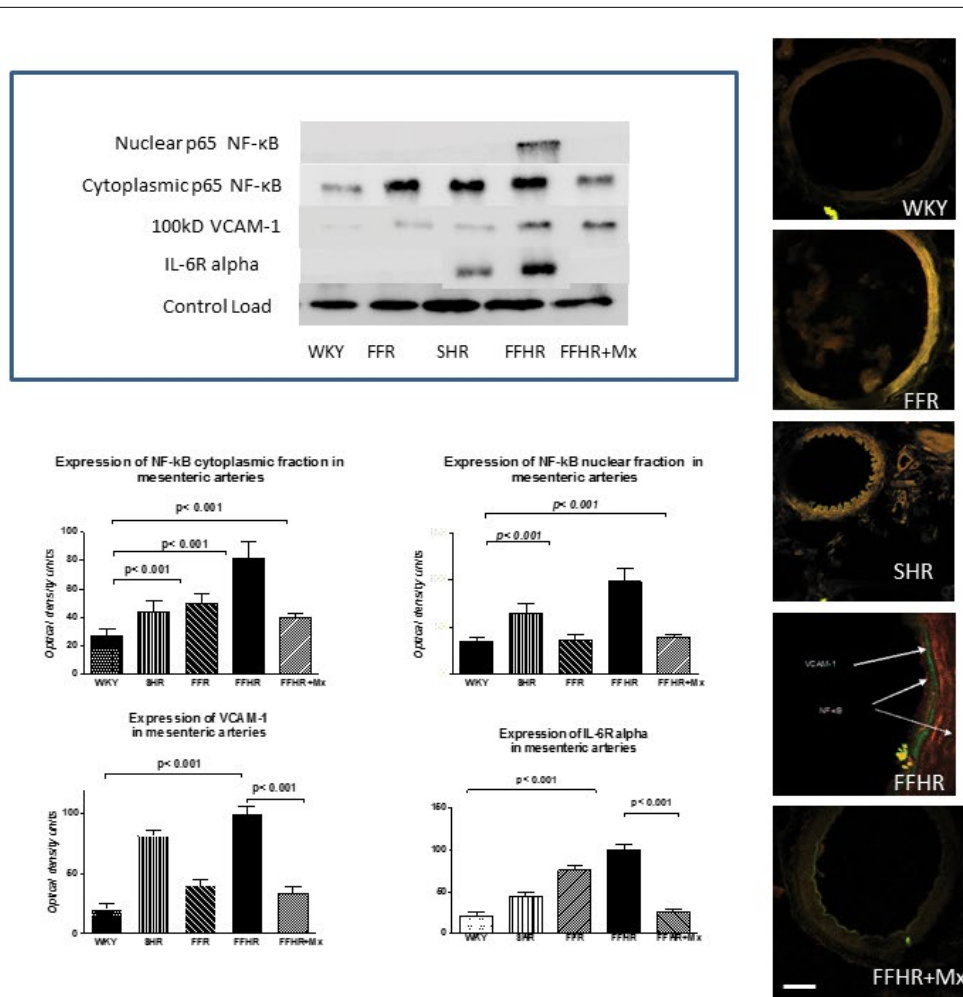


**Figure 1:** Cytoplasmic and nuclear p-65 fractions of NF- $\kappa$ B, VCAM-1 and IL-6 alpha expression in mesenteric arteries detected using WB and IHC. The upper panel shows a representative WB probed with anti-VCAM-1-FITC and anti-p65-TRITC. The graphs represent the optical density of the bands for each group. The lower panel shows microphotographs of mesenteric tissue obtained using a laser ICM 600x.

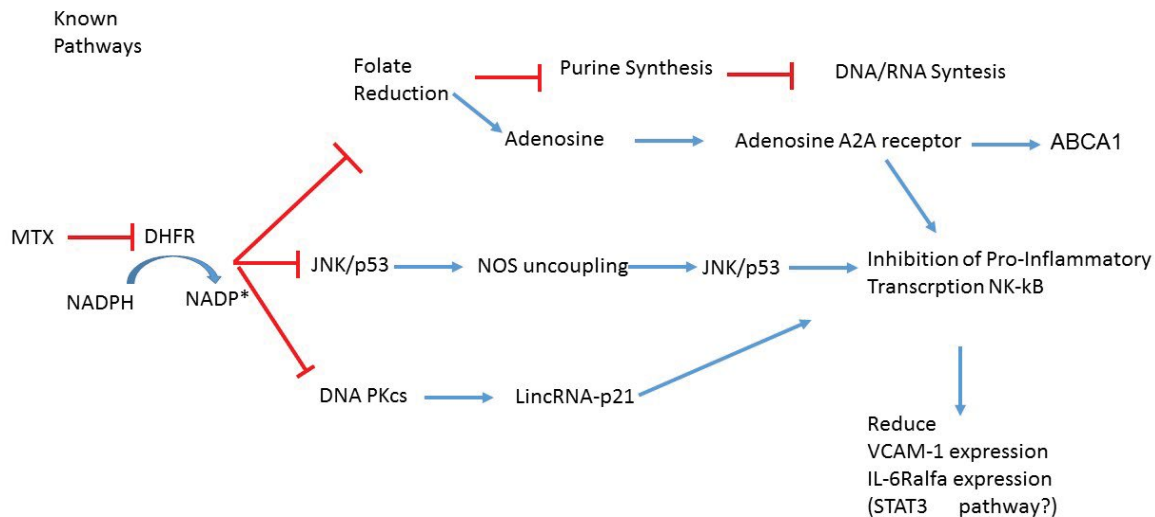


**Figure 2:** In this figure can be seen the mechanisms involved in the reduction of the expression of NF-κB, VCAM-1 and IL-6α. In addition, the pathway of adenosine is explained, which explains the modifications in the lipid profile as stated in the text.

induces the expression of key proteins in reverse cholesterol transport, including 27-hydroxylase and adenosine 5'-triphosphate-binding cassette transporter A1 (ABCA1), and prevents the formation of foam cells from human macrophages. A2A stimulation also attenuates inflammation and neointima formation after arterial injury in mice, and reduces expression of adhesion molecules commonly associated with the development of atheroma, such as vascular cell adhesion molecule-1 and intercellular adhesion molecule-1. Direct anti-inflammatory effects at the level of the vascular endothelium also likely have relevance; in New Zealand rabbits consuming a high cholesterol diet, weekly intravenous methotrexate administration reduced new atheroma formation by 75%, and led to a 2-fold reduction in the intima to media ratio and a marked reduction of macrophages and apoptotic cells within the aorta intima (Figure 2).

The FFHR experimental model develops hypertension, dyslipidaemia, insulin resistance, and vascular and cardiac remodelling. Inflammation in this model was demonstrated by increased hs-CRP and vascular inflammation due to increased expression of NF-κB, VCAM-1 and pro-atherogenic cytokines. The increased expression of VCAM-1 is a marker of vascular inflammation, vascular permeability, and endothelial dysfunction [16-18].

The inflammatory process identified in this experimental model has two components: 1- a local component involving an increase in the levels of nuclear transcription factors with subsequent activation of the inflammatory cascade that results in elevated cytokine levels and level 2- a systemic component involving increased hepatic synthesis of CRP due to a probable increase in IL-6 levels [10,13,19].

The development of a vascular microenvironment that is conducive to the creation, perpetuation, progression, and destabilization of vascular injury is either a simple eutrophic mechanism of vascular remodelling, or the generation of an atherosclerotic lesion [14,15,20].

A number of mechanisms may underlie these results. IL-6 is a well-established, independent indicator of multiple distinct types of cardiovascular disease and all-cause mortality. IL-6 is highly inducible in vascular tissues through the actions of the angiotensin II (Ang II) peptide, where it acts in a paracrine manner to signal through two distinct mechanisms; the first is a classic membrane receptor-initiated pathway, and the second is a trans-signalling pathway that induces responses even in tissues lacking the IL-6 receptor [21,22]. Recent advances and new concepts on how IL-6 receptor intracellular signalling pathways operate via the Janus kinase (JAK)-Signal Transducer and Activator of Transcription (STAT) have been described. IL-6 has diverse actions in multiple cell types of cardiovascular importance, including endothelial cells, monocytes, platelets, hepatocytes, and adipocytes. The central roles of IL-6 are in

endothelial dysfunction, cellular inflammation by affecting monocyte activation/differentiation, cellular cytoprotective functions from reactive oxygen species (ROS) stress, modulation of pro-coagulant state, myocardial growth control, and in metabolic control and insulin resistance. These multiple actions indicate that IL-6 is not merely a passive biomarker, but it actively modulates adaptive and pathological responses to cardiovascular stress [23,24].

Our observations elucidated previously unidentified broad cardiovascular effects [25] of MTX, which indicate a potential role of vascular inflammation modulators that can reduce the vascular complications of atherosclerosis-related metabolic syndrome. However, further research must be performed to understand if the subunit gp130 or inhibition of STAT3 directly produces anti-inflammatory and anti-angiostensin effects.

## Acknowledgement

The authors have no conflict of interest to report.

## References

1. Almalag HM, Mangoni AA, Crilly MA (2012) Methotrexate and risk of cardiovascular disease. *Am J Cardiol* 109: 1383-1384.
2. Vilsbøll T, Knop F, Krarup T, Johansen A, Madsbad S, et al. (2003) The Pathophysiology of Diabetes Involves a Defective Amplification of the Late-Phase Insulin Response to Glucose by Glucose-Dependent Insulinotropic Polypeptide-Regardless of Etiology and Phenotype. *J Clin Endocrinol Metab* 88: 4897-4903.
3. Timper K, Grisouard J, Sauter NS, Herzog-Radimersk T, Dembinski K, et al. (2013) Glucose-dependent insulinotropic polypeptide induces cytokine expression, lipolysis and insulin resistance in human adipocytes. *Am J Physiol Endocrinol Metab* 304.
4. Renna NF, Lembo C, Diez E, Miatello RM (2013) Role of Renin-Angiotensin system and oxidative stress on vascular inflammation in insulin resistance model. *Int J Hypertens* 2013: 420979.
5. Valerio A, Cardile A, Cozzi V, Bracale R, Tedesco L, et al. (2006) TNF-α downregulates eNOS expression and mitochondrial biogenesis in fat and muscle of obese rodents. *J Clin Invest* 116: 2791-2798.
6. Vomhof-DeKrey EE, Picklo MJ (2012) NAD(P)H:quinone oxidoreductase 1 activity reduces hypertrophy in 3T3-L1 adipocytes. *Free Radic Biol Med* 53: 690-700.
7. Barnett A (2006) DPP-4 inhibitors and their potential role in the management of type 2 diabetes. *Int J Clin Pract* 60: 1454-1470.
8. Furchgott RF, Zawadzki JV (1980) The obligatory role of endothelial cells in the relaxation of arterial smooth muscle by acetylcholine. *Nature* 288: 373-376.
9. Ignarro L, Byrns R, Buga G, Wood K (1987) Endothelium-derived relaxing factor from pulmonary artery and vein possesses pharmacologic and chemical properties identical to those of nitric oxide radical. *Circ Res* 61: 866-879.
10. Renna NF, Vazquez MA, Lama MC, González ES, Miatello RM (2009) Effect of chronic aspirin administration on an experimental model of metabolic syndrome. *Clin Exp Pharmacol Physiol* 36: 162-168.

11. Keaney JF, Gaziano JM, Xu B, Frei B, Curran-Celentano J, et al. (1993) Dietary Antioxidants Preserve Endothelium-Dependent Vessel Relaxation in Cholesterol-Fed Rabbits. *Proc Natl Acad Sci U S A* 90: 11880-11884.
12. Fleming I, Busse R (1999) Signal transduction of eNOS activation. *Cardiovasc Res* 43: 532-541.
13. Renna NF, Diez ER, Lembo C, Miatello RM (2013) Role of Cox-2 in vascular inflammation: an experimental model of metabolic syndrome. *Mediators Inflamm* 2013: 513251.
14. Renna NF, Diez EA, Miatello RM (2014) Effects of dipeptidyl-peptidase 4 inhibitor about vascular inflammation in a metabolic syndrome model. *PLoS One* 9: e106563.
15. Nikolaidis LA, Mankad S, Sokos GG, Miske G, Shah A, et al. (2004) Effects of glucagon-like peptide-1 in patients with acute myocardial infarction and left ventricular dysfunction after successful reperfusion. *Circulation* 109: 962-965.
16. Peairs AD, Rankin JW, Lee YW (2011) Effects of acute ingestion of different fats on oxidative stress and inflammation in overweight and obese adults. *Nutr J* 10: 122.
17. Dong A, Shen J, Zeng M, Campochiaro PA (2011) Vascular cell-adhesion molecule-1 plays a central role in the proangiogenic effects of oxidative stress. *Proc Natl Acad Sci U S A* 108: 14614-14619.
18. Renna NF, de Las Heras N, Miatello RM (2013) Pathophysiology of vascular remodeling in hypertension. *Int J Hypertens* 2013: 808353.
19. Siegel D, Swislocki AL (2007) Effects of antihypertensives on glucose metabolism. *Metab Syndr Relat Disord* 5: 211-219.
20. Kim J, Won JS, Singh AK, Sharma AK, Singh I (2014) STAT3 regulation by S-nitrosylation: implication for inflammatory disease. *Antioxid Redox Signal* 20: 2514-2527.
21. Verweij SL, van der Valk FM, Stroes ES (2015) Novel directions in inflammation as a therapeutic target in atherosclerosis. *Curr Opin Lipidol* 26: 580-585.
22. Kovacic J, Gupta R, Lee AC, Ma M, Fang F, et al. (2010) Stat3-dependent acute Rantes production in vascular smooth muscle cells modulates inflammation following arterial injury in mice. *J Clin Invest* 120: 303-314.
23. Brasier AR (2010) The nuclear factor-kappaB-interleukin-6 signalling pathway mediating vascular inflammation. *Cardiovasc Res* 86: 211-218.
24. Shah Z, Kampfrath T, Deiluiis JA, Zhong J, Pineda C, et al. (2011) Long-Term Dipeptidyl-Peptidase 4 Inhibition Reduces Atherosclerosis and Inflammation via Effects on Monocyte Recruitment and Chemotaxis. *Circulation* 124: 2338-2349.
25. Hou T, Tieu BC, Ray S, Recinos Iii A, Cui R, et al. (2008) Roles of IL-6-gp130 Signaling in Vascular Inflammation. *Curr Cardiol Rev* 4: 179-192.